Growth and characterization of $Fe_{1-x}Ga_x$ thin films from citrates-based electrolytes

R. Ranchal and D. Maestre

Dpto. Física de Materiales, Facultad de Ciencias Físicas. Universidad Complutense de Madrid. Ciudad Universitaria s/n, Madrid 28040, Spain

Abstract

In this work we report on the growth of $Fe_{1-x}Ga_x$ films by means of the electrodeposition technique in baths containing sodium citrate as an antioxidant agent. We have investigated the effect of the electrolyte composition in terms of its Ga content on the structural and magnetic properties. Our experimental results indicate that for the optimized bath composition, O-free $Fe_{1-x}Ga_x$ alloys can be achieved for a potential of E = -1.4 V and magnetic stirring at 500 rpm. Both, the composition and the coercivity of the samples deposited from this electrolyte can be tuned by means of the duration of the rest pulse at E = -1.12 V. However, when the composition of the bath is not optimized the films exhibit a large amount of O that cannot be dissolved during the rest pulse. Our experimental results show that O-free $Fe_{1-x}Ga_x$ alloys with a Ga content around 19 at. % and optimum magnetic properties can be deposited on Au substrates when using an optimized electrolyte and long rest pulses.

Keywords: FeGa alloys; electrodeposition; magnetic properties.

Contact autor

Dr. R. Ranchal

Dpto. Física de Materiales, Facultad Ciencias Físicas. Universidad Complutense de Madrid.

Ciudad Universitaria s/n Madrid 28040, Spain.

Phone: 00 34 91 394 5012

Fax: 00 34 91 394 4547

e-mail: rociran@ucm.es

1. Introduction

In the last years, $Fe_{1-x}Ga_x$ alloys have received great attention due to their unique magnetoelastic properties [1-10]. The magnetostriction constant (λ_s) for these alloys shows two peaks for Ga contents around 19 at. % and 30 at. % [8]. Besides, the exact position of these peaks depends on the thermal history during the processing and higher magnetostriction values are achieved for the quenched samples at Ga contents of 18 and 28 at. % [8]. However, it is necessary to develop industrial processes to produce these alloys and the electrodeposition appears as an interesting option as it is a feasible and cheap technique. In the industry this technique is widely used to deposit high quality films with thicknesses from few microns to few nanometers.

Increasing research efforts have been recently invested in the growth of $Fe_{1-x}Ga_x$ films by means of the electrodeposition [11-18]. One of the challenges of this technique is the non desirable and hardly avoidable formation of oxides and/or hydroxides. In the literature, two basic electrolytes are found to overcome this drawback. In one electrolyte boric acid is used to reduce the oxidation, while ascorbic acid is employed as antioxidant of the Fe ions from Fe^{2+} to Fe^{3+} [11-14]. In this case, the pH of the electrolyte must be around 2. In the other electrolyte, just sodium citrate is used as antioxidant and the pH can be increased up to 4 [15-18]. This higher pH enables to reduce the H_2 evolution, as during electrodeposition of $Fe_{1-x}Ga_x$ alloys voltages more negative than the hydrogen reduction are necessary. Moreover, due to its three possible ionic states (-1, -2 and -3), the citrate can form stable complexes with both Fe^{2+} and Ga^{3+} avoiding their oxidation.

Another important issue in the $Fe_{1-x}Ga_x$ alloys is the correlation between structural and magnetostrictive properties. As mentioned above, the λ_s exhibits two peaks at Ga concentrations of 18 and 28 % in the <100> direction for quenched bulk

samples [8]. Therefore, although it is convenient to deposit <100> textured films the $Fe_{1-x}Ga_x$ alloys exhibit a tendency to the <110> texture when grown by either electrodeposition or vacuum techniques [12, 16, 19-21]. It has been reported that the <100> texture can be enhanced when electrodepositing on <100>-oriented GaAs substrate [17] but it is desirable to extend this result to other substrates. In this work we have investigated the growth of $Fe_{1-x}Ga_x$ thin films from electrolytes based on sodium citrate and in particular, we have studied the influence of the electrolyte composition and duration of the rest pulse on the composition and magnetic properties of the as grown alloys deposited on Au substrates.

2. Experimental details

Si(100) wafers coated with Ta(30 nm), Cu (120 nm) and Au (20 nm) layers were used as working electrodes. Then, the $Fe_{1-x}Ga_x$ films were deposited on top of the upper Au layer. Experiments were carried out in two electrolytes with different Ga^{3+} content. The first one (named as electrolyte A) consists of an aqueous solution of 35 mM Na_3-citrate, 15 mM $FeSO_4 \cdot 7\ H_2O$, 15 mM $Ga_2(SO_4)_3 \cdot 18\ H_2O$, mixed in this order. In the second electrolyte (named as electrolyte B), the concentration of $Ga_2(SO_4)_3$ is increased up to 35 mM, being the composition of this electrolyte an aqueous solution of 35 mM Na_3-citrate, 15 mM $FeSO_4 \cdot 7\ H_2O$ and 35 mM $Ga_2(SO_4)_3 \cdot 18\ H_2O$, mixed in this order. Hence, according to the initial compositions, the amount of Ga is higher in electrolyte B than in electrolyte A. In all cases, the pH was adjusted to 4 by adding diluted NH_4OH (10% vol.). Moreover, citrate-containing electrolytes usually have a low current efficiency [22-23] and ammonia is commonly added to the baths in order to overcome this problem. For each experiment 40 ml of fresh electrolyte was used. A Pt sheet was used as the counter electrode and a Ag/AgCl as the reference electrode. Deposition

experiments were carried out using an Ecochemie potentiostat/galvanostat AUTOLAB PG-STAT30. All experiments were carried out at room temperature and the electrolyte was continuously agitated with a magnetic stirring at 500 rrpm. The substrate is immersed in the cell without applying any potential measuring an open circuit potential of few mV. After finishing the growth, the potential control is stopped and the sample is immediately extracted from the electrolyte.

The growth rate has been inferred considering the thickness of the layers and the total time of growth for each sample. To measure the thickness of the layers we create a sharp step by means of optic lithography followed by a chemical etching. The height of this step is the thickness of the layer that is directly measured in an Alphastep profiler. The thickness has been measured in several parts of the step to confirm that the layer is homogenous. X-ray diffractometry (XRD) in the Bragg-Brentano configuration was performed in a Phylips X'Pert MPD using the Cu K_α wavelength (1.54056 Å). The composition of the samples was analyzed by means of the Energy Dispersive X-ray Spectroscopy (EDS) in a Leica 440 scanning electron microscope (SEM) operated at 8 kV and 1.5 nA. The in-plane hysteresis loops were carried out in a vibrating sample magnetometer (VSM) from LakeShore at room temperature.

3. Results and discussion

To analyze the codeposition process of Fe and Ga we have performed potentiodynamic current-potential curves at a scan rate of 10 mV/s (Figure 1.a). Theoretically, the reduction of Ga^{3+} and Fe^{2+} takes place at potentials of E = -0,78 V and E = -0.63 V respectively. No significant current variations are observed in the potential range from -0.4 V to -1.0 V for the electrolyte B, while electrolyte A shows a clear increase of the current in this potential range that could indicate Ga^{3+} and Fe^{2+}

reduction. Hence, the reduction of those ions seems to be significant in that potential regime for electrolyte A, whereas that is not the case for the B. It is also important to remark that in spite of the lower concentration of Ga^{3+} in the electrolyte A, the current density in this electrolyte is higher in the whole overpotential regime studied in this work (fig 1a) and therefore, more reduction processes should be taken place in this electrolyte. The high increase of the current observed in the two electrolytes at around -1 V corresponds to the H_2O reduction. At around -1.17 V a change of slope can be observed in the curve of the electrolyte B (indicated with an arrow in Figure 1a) but it is not so evident for electrolyte A. This potential is similar to the value reported by Reddy et al. [18] at which $Fe_{1-x}Ga_x$ alloys can start to be deposited (E > -1.18 V). Moreover, in the two electrolytes we have observed that stable deposits are only achieved for potentials equal or more negative than E ~ -1.17 V. Therefore, taking into account all these results, we have selected a growth pulse of E = -1.4 V because is higher than the values at which stable deposits are obtained and a similar value has been successfully used in a previous work [13]. For the rest potential we have chosen a value of E = -1.12 V that it is just below the potential at which there is a change of slope and at which a proper growth of $Fe_{1-x}Ga_x$ seems to start (E =-1.17 V), as inferred from the current-potential curves. Actually, potentials around this value have already been reported to effectively dissolve the hydroxides formed during the growth of $Fe_{1-x}Ga_x$ alloys in boric and ascorbic electrolytes [11]. The growth pulse has been fixed to 2 s and different samples have been obtained by increasing the duration of the rest pulse from zero (continuous sample) to 8 s. By continuous sample we mean a sample deposited in the continuous mode, i.e. the duration of the rest pulse is zero. A typical behavior of the current measured during the growth of the samples can be found in the inset of figure 1 (a).

The continuous layers have a similar growth rate for the two electrolytes (Figure 1 (b)). In both electrolytes the growth rate decreases with the duration of the rest pulse but it reaches a different steady value for each one. The lower growth rate observed for the pulsed samples, even for a duration of 0.5 s, as compared to the continuous ones, demonstrates that the layers are effectively dissolved during the rest pulse for both electrolytes (fig. 1 b). The steady growth rate achieved in the two cases indicates that the increase of the duration of the rest pulse above 0.5 s does not further enhance the dissolution of the $Fe_{1-x}Ga_x$ layers. However, the higher growth rate reached in the pulsed layers from electrolyte A indicates that there are more reduction processes in that electrolyte in spite of its lower concentration of Ga^{3+}. This is also in agreement with the larger current density measured in the current-potential curves corresponding to that electrolyte (Figure 1a). The number of pulses varies between 90 and 130. In figure 1 (c) and (d) we present several cyclic voltammetries (CV) for the two electrolytes. The electrolyte B can be used during several pulses as we have not observed a significant deterioration of the electrolyte. However, electrolyte A seems not to be so adequate.

The layers obtained from the two electrolytes are polycrystalline as evidenced by the diffraction patterns (Fig. 2). In all the samples, there appear different diffraction peaks close to those related to α-Fe as it has been reported in bulk $Fe_{1-x}Ga_x$ alloys or thin films deposited from vacuum techniques [7, 9, 19]. Assuming a cubic structure, the calculated lattice parameters for the $Fe_{1-x}Ga_x$ alloys are higher than those of α-Fe, indicating the introduction of Ga in the Fe lattice as expected in this kind of alloys in the form of thin films [19]. The calculated lattice parameters are higher for the samples deposited from electrolyte B ($a \sim 2.89$ Å) than for A ($a \sim 2.87$ Å) which might indicate that a larger amount of Ga has been introduced in the former samples. It is difficult to extract information about the presence of crystalline FeGaO based on the study of the

XRD patterns, as for example, one of the diffraction peaks of this oxide is close to one of Ta ($2\theta \sim 32.9°$). Therefore, the existence of FeGaO compounds cannot be rule out from XRD characterization. The presence of the (200) and (110) diffraction peaks in the patterns indicate <100> and <110> texture in our samples. However, Ga contents about 19 at. % or 30 at. % are also required in order to ensuing magnetostrictive performance.

We have measured the composition of the samples by the EDS technique in a SEM. Figure 3a shows characteristic EDS spectra (raw data) acquired from representative samples deposited from electrolyte A and B. The influence of the duration of the rest pulse on the Ga, Fe and O content measured from EDS spectra is shown in Figures 3b-d. Due to the thickness of the samples (300 – 400 nm), occasionally small peaks corresponding to Au or Cu from the substrate are also detected by EDS, although they have not been quantitative analyzed. The amount of Ga detected by EDS is around three times higher in all the samples grown from electrolyte B due to the higher Ga^{3+} concentration in this electrolyte (Fig. 3(b)). The average levels of Ga detected by EDS (Ga ~ 19 at. %) in the layers deposited from electrolyte B and the range of the corresponding lattice parameters (a ~ 2.89 Å) are in agreement with the values of Ga content and the corresponding lattice parameters previously reported in sputtered films with similar Ga contents [19]. For layers deposited from A, the Ga content is around 6 at.% and the average lattice parameter inferred for those layers is a slightly higher in comparison with the values reported by Dunlap et al. [19]. In both electrolytes the Ga content decreases with the duration of the rest pulse (figure 3b), that ranges from 0 s to 8 s, while the opposite behaviour is observed in the evolution of the Fe content with the duration of the rest pulse (figure 3c), revealing that Ga is more effectively dissolved than Fe during the rest pulse (E = - 1.12 V). This is further suggested by the fact that the increase of Fe with the duration of the rest pulse seems to

be complementary to the decrease of Ga with this parameter (Fig. 3 (b) and (c)). It is significant that the Ga and Fe compositions in the layers do not correspond to the composition of the corresponding electrolyte. Although the Ga^{3+} in both electrolytes is higher than that of Fe^{2+}, there is a higher Fe content than Ga in the layers (Fig. 3 (b) and (c)). Also, the difference of Ga content between the layers, around three times higher for samples obtained from bath B, does not correspond with the difference in the Ga concentration between the electrolytes, which is around two times higher for electrolyte B. Finally, is it important to consider the big difference of O in the samples deposited from each electrolyte (Fig. 3 (d)). Layers from electrolyte A have a large amount of O, around 25 at. %, whereas in the samples from electrolyte B we have only detected a 5 at. % of O. Considering that the films were uncapped, this O content of 5 at. % can be correlated to surface oxidation or to oxygen stemming from the substrate. In order to confirm this point, we have also measured by EDS the O content in the pristine substrate and we have detected values lower than 6 at.%. Hence, samples from electrolyte B can be considered as free of hydroxides and FeGaO phases but not the layers deposited from A. On the other hand, the large amount of O observed in the samples from electrolyte A can explain the different lattice parameter inferred in those samples in comparison with previously sputtered samples with the same composition [19]. Finally, if we consider the requirements regarding the necessity of a Ga content close to the 19 at. % and low O concentration, all of them can be achieved when using the electrolyte B and a long rest pulse between 4 and 8 s.

K. S. Reddy et al., proposed a mechanism of co-deposition in which different partial reductions of Fe^{2+} and Ga^{3+} ions together with the formation of different adsorbed species take place [18]. K. S. M. Reddy et al., proposed the following codeposition process for Fe and Ga:

$$Fe(II) + e^- \rightarrow [Fe(I)]_{ads} \quad (I)$$

$$[Fe(I)]_{ads} + e^- \rightarrow Fe(s) \quad (IIa)$$

$$[Fe(I)]_{ads} + Ga(III) \rightarrow [Ga(III)—Fe(I)]_{ads} \quad (IIb)$$

$$[Ga(III) —Fe(I)]_{ads} + 3\ e^- \rightarrow Ga(s) + [Fe(I)]_{ads} \quad (IIc)$$

In this codeposition process it is necessary to avoid the formation of low valence Ga ions that when reacting with oxygen leads to the formation of FeGaO phases instead of $Fe_{1-x}Ga_x$ alloys. It is reported that this can be achieved by either rotating the substrate at a sufficient velocity (ω > 200 rpm) or selecting appropriate growth potentials for the growth (E > -1.18 V) [18]. As we have already discussed, we observe a change of slope around this potential in our current-potential curves being more evident in the electrolyte B (Fig. 1a). Thus, the codeposition process is more favourable in bath B. After the first reaction of the codeposition process (step I), the adsorbed Fe^{1+} ion can be reduced to metallic Fe (step IIa) or follow the route to produce $Fe_{1-x}Ga_x$ alloys after the formation of an adsorbed complex between $[Fe(I)]_{ads}$ and $[Ga(III)]_{ads}$ (step IIb). This process explains why the Ga content in the layers is much smaller in comparison to the electrolyte concentration because if the step (IIa) is followed, only metallic Fe (and not Ga) is incorporated in the films. In electrolyte B the quantity of Ga^{3+} ions is two times higher than in A. Then, the probability of the step (IIb) that produces O-free $Fe_{1-x}Ga_x$ alloys is also two times higher in this electrolyte. This can be observed in the current-density curves as the change of slope around E = -1.17 V is more evident for electrolyte B. In the electrolyte A, it seems to exist another route, apart from the codeposition process proposed by Reddy et al., that promotes the incorporation of O in the samples. In electrolyte A there are reduction processes that occur at potentials between -0.4 V and -1 V that can take place during the rest potential (E = -1.12 V) which are not observed for electrolyte B (fig. 1 a). These reactions, which are not considered in the

normal codeposition process, could be the reason of the observed O incorporation in the samples deposited from electrolyte A. Furthermore, these reactions can explain both the higher current density and steady growth rate obtained in electrolyte A because more reductions processes are taken place in comparison to B.

The experimental results also indicate that the FeGaO phases cannot be fully dissolved during the rest pulse used in this work (E = -1.12 V) when using bath A. This can be explained considering that the rest potential is more negative than the reduction processes that introduced the O in our samples, those between -0.4 and -1.0 V. The data presented in this work also show that in electrolyte B the magnetic stirring at 500 rpm and a growth potential of -1.4 V enable the growth of layers apparently free of FeGaO phases. Nevertheless, a large amount of O is introduced in the layers when the same conditions are used in the electrolyte A. The low O content, associated with surface oxidation observed in the continuous layer indicates that for electrolyte B it is not necessary the rest pulse for the dissolution of possible hydroxides because actually they are not formed during the growth at -1.4 V when this bath is used for the growth of the samples. Therefore, in this optimized electrolyte B the oxygen-free codeposition process proposed by Reddy takes place during the growth of the samples. Moreover, only with this electrolyte we can obtain $Fe_{1-x}Ga_x$ alloys with $15 \leq x \leq 22$ being possible to tune the Ga content around the 19 at. %, composition at which the magnetostriction of these alloys exhibits one peak [8].

In figure 4 we present the hysteresis loops recorded for all the studied samples. Comparing these two graphs we can infer that both lower coercivity and lower saturating fields are obtained in samples from electrolyte B. In figure 5 (a) we present the coercivity (H_C) inferred from those loops at room temperature as a function of the Ga content. In both cases, the H_C decreases as the Ga content is also reduced. However,

much lower H_C values can be achieved when using the bath B. This difference can be due to two main reasons. On one hand, the Ga content in the samples obtained from B is around three times higher than in the samples A and it is known that the introduction of Ga helps to reduce the coercivity. On the other, the amount of O is much higher in samples A and this can also increase the H_C. O-free layers can be achieved growing in the continuous mode and using the electrolyte B. However, the introduction of rest pulses enables to tune both the composition [Fig. 3] and the coercive field of the films [Fig. 5 (a)]. For the optimized electrolyte B, coercivities from 28 to 16 Oe can be obtained for the rest pulses studied in this work. Moreover, H_C is around 23 Oe for a Ga content of 19 at. %. However, just low coercivity values cannot be used to warrant a high quality in our $Fe_{1-x}Ga_x$ samples. In figure 5 (b) we have plotted the saturation magnetization (M_s) as a function of the Ga content for the two electrolytes. In samples from A, the M_s decreases with the Ga content. This fact points out that the Ga is not correctly introduced in the Fe lattice and actually, it can also explains the increase of coercivity with the Ga content observed in this series of samples. On the other hand, layers obtained from B exhibit higher M_s values in the Ga content range around the 19 at. %. The results of figure 5 show that layers from electrolyte B with a Ga content around 19 at. % have a M_s of 1290 emu/cm^3 and a H_C of 23 Oe. Therefore, our experimental results show that O-free $Fe_{1-x}Ga_x$ alloys with a Ga content around 19 at. % and optimum magnetic properties can be deposited on Au substrates when using the electrolyte B and long rest pulses between 4 and 8 s.

4. Conclusions

We have investigated the influence of the electrolyte composition on the composition and magnetic properties of $Fe_{1-x}Ga_x$ films obtained from citrates-based

electrolytes. We have also analyzed the influence of the duration of the rest pulse on these layers characteristics. It is necessary to adjust the electrolyte composition because FeGaO phases can appear even when the growth potential and the speed for the magnetic stirring are regulated. In the non-optimized electrolyte A, FeGaO phases are difficult to dissolve during the rest pulses at E = -1.12 V. The optimized electrolyte B enables to obtain $Fe_{1-x}Ga_x$ alloys, $15 \leq x \leq 22$, being possible to tune the Ga content around the 19 at. %, composition, by means of the rest pulse. The coercivity and saturation magnetization can also be further adjusted being possible to obtain O-free $Fe_{1-x}Ga_x$ alloys with a Ga content around 19 at. %, and optimum magnetic properties on Au substrates when using an optimized electrolyte and long rest pulses.

Acknowledgements. This work has been financially supported through the projects MAT2011-28751-C02 and MAT 2012-31959 of the Spanish Ministry of Science and Innovation. We thank “CAI Difracción de rayos-X” of UCM for the x-ray diffractometry measurements.

References

[1] A. E. Clark, J. B. Restorff, M. Wun-Fogle, T. A. Lograsso, and D. L. Schlagel, IEEE Trans. Magn. 36 (2000) 3238.

[2] A. E. Clark, M. Wun-fogle, T. A. Lograsso, and J. R. Cullen, IEEE Trans. Magn. 37 (2001) 2678.

[3] M. Laver, C. Mudivarthi, J. R. Cullen, A. B. Flatau, W.-C. Chen, S. M. Watson, and M. Wuttig, Phys. Rev. Lett. 105 (2010) 027202.

[4] M. P. Ruffoni, S. Pascarelli, R. Grössinger, R. Sato Turtelli, C. Bornio-Nunes, and R. F. Pettifer, Phys. Rev. Lett. 101 (2008) 147202.

[5] H. Cao, P. M. Gehring, C. P. Devreugd, J. A. Rodriguez-Rivera, J. Li, and D. Viehland, Phys. Rev. Lett. 102 (2009) 127201.

[6] E. Arenholz, G. van der Laan, A. McClure, and Y. Idzerda, Phys. Rev. B 82 (2010) 180405.

[7] O. Ikeda, R. Kainuma, I. Ohnuma, K. Fukamichi, and K. Ishida, J. Alloys Compnd. 347 (2002) 198.

[8] Q. Xing, Y. Du, R. J. McQueeney, and T. A. Lograsso, Acta Materialia 56 (2008) 4536.

[9] H. Cao,F. Bai, J. Li, D. Viehland, T.A.Lograsso, and P. M. Gehring, J. Alloys Compnd. 465 (2008) 244.

[10] M. Barturen, B. RacheSalles, P. Schio, J.Milano, A.Butera, S. Bustingorry, C. Ramos, A.J.A. de Oliveira, M. Eddrief, E. Lacaze, F. Gendron, V. H. Etgens, and M. Marangolo, Appl.Phys. Lett. 101 (2012) 092404.

[11] D. Iselt, K. Tschulik, S. Oswald, D. Pohl, L. Schultz, and H. Schlörb, J. Electrochemical Society 159 (2012) H633.

[12] D. Iselt, U. Gaizsch, S. Oswald, S. Fähler, L. Schultz, amd H. Schlörb, Electrochimica Acta 56 (2011) 5178.

[13] D. Iselt, A. Funk, L. Schultz, and H. Schlorb, ECS Electrochemistry Lett. 2 (2013) D13.

[14] N. Lupu, H. Chiriac, and P. Pascariu, J. Appl. Phys. 103 (2008) 07B511.

[15] P. D. McGary, K. S. M. Reddy, G. D. Haugstad, and B. J. H. Stadler, J. Electrochemical Society, 157 (2010) D656.

[16] S. M. Reddy, J. J. Park, S. M. Na, M. M. Maqableh, A. B. Flatau, and B. J. H. Stadler, Advanced Functional Materials 21 (2011) 4677.

[17] K. S. Madhukar Reddy, M. Maqablesh, and B. J. H. Stadler J. Appl. Phys. 111 (2013) 07E502.

[18] K. S. M. Reddy, E. C. Estrine, D.-H. Lim, W. H. Smyrl, and B. J. H. Stadler, Electrochemistry Communications 18 (2013) 127.

[19] R. A. Dunlap, N. C. Deschamps, R.E. Mar, and S. P. Farrell, J. Phys.: Conden. Matter. 18 (2006) 4907.

[20] N. A. Morley, A. Javed, and M. R. Gibbs, J. Appl. Phys. 105 (2009) 07A912.

[21] R. R. Basantkumar, B. J. H. Stadler, W. P. Robinson, and E. M. Summers, IEEE Trans. Magn. 42 (2006) 3102.

[22] I. Mizushima, P.T. Tang, H.N. Hansen, M.A.J. Somers, Electrochimica Acta, 51 (2006) 6128.

[23] M.A.M. Ibrahim, S.S. Abd El Rehim, S.O. Moussa, J. Appl. Electrochem., 33 (2003) 627.

Figure captions.

Figure 1. (a) Current-potential curves for the two electrolytes. (b) Growth rate as a function of the rest pulse for the electrolytes A (●) and B (○). Cyclic voltammetries showing the first and the sixth scan for electrolyte A (c) and B (d). Color on line.

Figure 2. Diffraction patterns of the samples obtained from electrolyte A, graph (a) and from electrolyte B, graph (b). In each curve it is displayed the duration of the rest pulse. Color on line.

Figure 3. (a) EDS spectra characteristic from electrolyte A and B showing peaks corresponding to Fe, Ga and O. In graphs (b), (c), and (d) it is displayed the Ga, Fe, and O content as a function of the rest pulse, respectively. In all the graphs, samples obtained from electrolyte A are represented by solid circles (●), and by open circles (○) for films obtained from electrolyte B. The dashed lines are guides to the eye. Color on line.

Figure 4. Hysteresis loops recorded at room temperature for all the studied samples. Samples from electrolyte A (a) and from electrolyte B (b). The insets of each graph display the low field region. Color on line.

Figure 5. (a) Coercive field at room temperature as a function of the Ga content and (b) saturation magnetization also at room temperature as a function of the Ga content. In both cases, (●) closed circles are used for samples deposited from electrolyte A and (○) open circles are used for layers obtained from electrolyte B. The dashed lines are guides to the eye. Color on line.

Figure 1

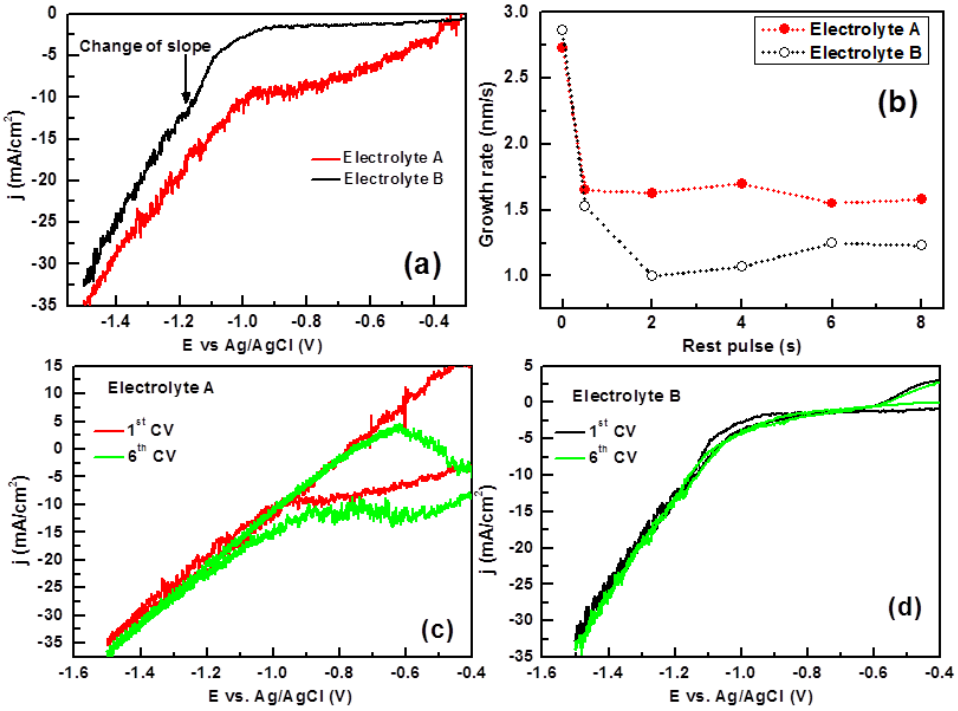
Change of slope
Electrolyte A
Electrolyte B
(a)
j (mA/cm²)
E vs Ag/AgCl (V)
Growth rate (nm/s)
Rest pulse (s)
(b)
Electrolyte A
1st CV
6th CV
(c)
E vs. Ag/AgCl (V)
Electrolyte B
(d)

Figure 2

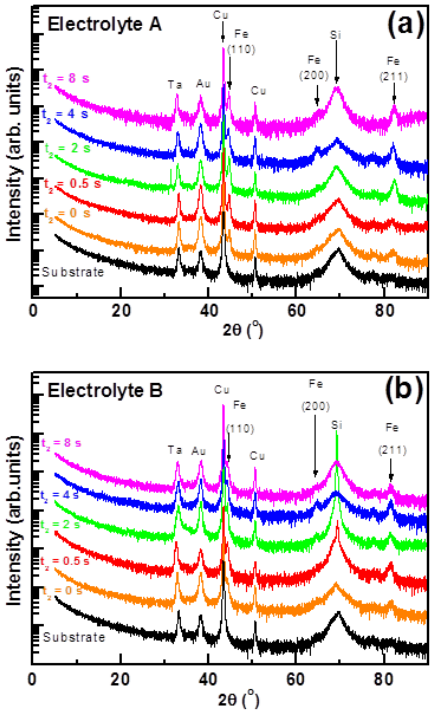
Electrolyte A
(a)
Cu
Fe
(110)
Si
Fe
(200)
Fe
(211)
Ta
Au
Cu
t_z = 8 s
t_z = 4 s
t_z = 2 s
t_z = 0.5 s
t_z = 0 s
Substrate
Intensity (arb. units)
0
20
40
60
80
2θ (°)
Electrolyte B
(b)
Cu
Fe
(110)
Fe
(200)
Si
Fe
(211)
Ta
Au
Cu
t_z = 8 s
t_z = 4 s
t_z = 2 s
t_z = 0.5 s
t_z = 0 s
Substrate
Intensity (arb.units)
0
20
40
60
80
2θ (°)

Figure 3

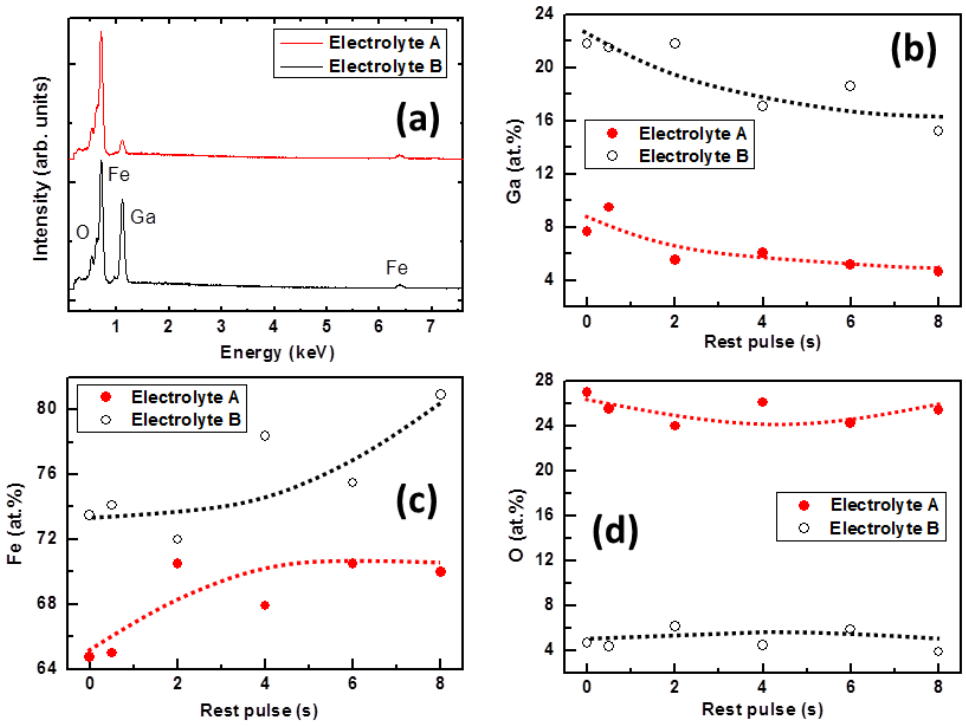
Electrolyte A
Electrolyte B
(a)
Intensity (arb. units)
Fe
Ga
O
Fe
Energy (keV)
(b)
Ga (at.%)
Rest pulse (s)
(c)
Fe (at.%)
Rest pulse (s)
(d)
O (at.%)
Rest pulse (s)

Figure 4

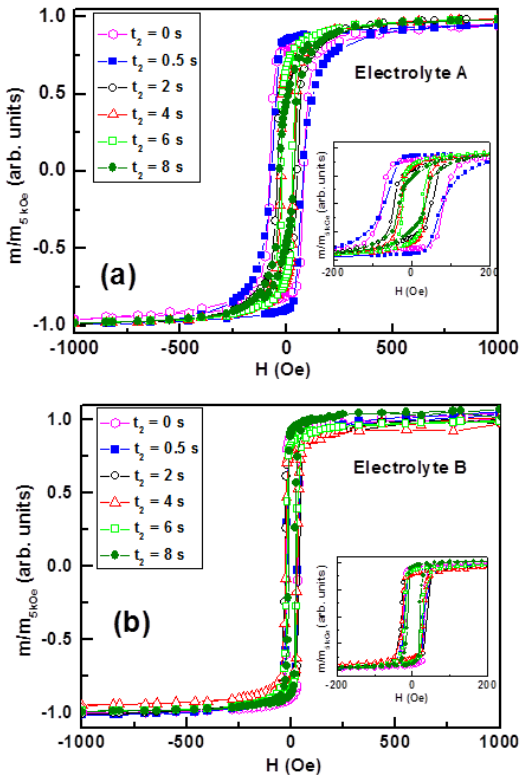
t2 = 0 s
t2 = 0.5 s
t2 = 2 s
t2 = 4 s
t2 = 6 s
t2 = 8 s
Electrolyte A
(a)
m/m5KOe (arb. units)
H (Oe)
Electrolyte B
(b)

Figure 5

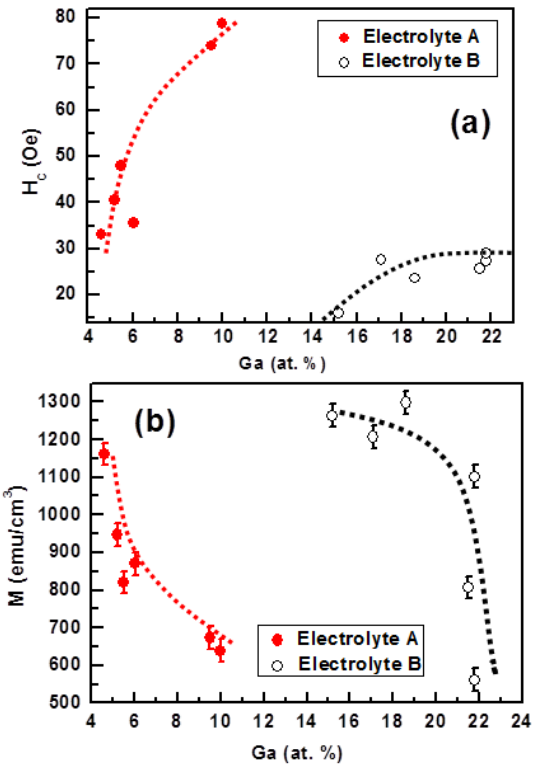
Electrolyte A
Electrolyte B
(a)
H_c (Oe)
Ga (at. %)
(b)
M (emu/cm^3)
Electrolyte A
Electrolyte B
Ga (at. %)